Rituximab (anti-CD20) selectively modifies Bcl-xL and apoptosis protease activating factor-1 (Apaf-1) expression and sensitizes human non-Hodgkin's lymphoma B cell lines to paclitaxel-induced apoptosis

Ali R. Jazirehi,[1,2] Xiao-Hu Gan,[1] Sven De Vos,[3] Christos Emmanouilides,[3] and Benjamin Bonavida[1]

[1]Department of Microbiology, Immunology and Molecular Genetics, [2]Department of Oral Biology and Medicine, School of Dentistry, and [3]Department of Hematology and Oncology, Jonsson Comprehensive Cancer Center, David Geffen School of Medicine at UCLA, University of California, Los Angeles, CA

Abstract

The anti-CD20 monoclonal antibody rituximab (Rituxan, IDEC-C2B8) has shown promising results in the clinical treatment of a subset of patients with low grade or follicular non-Hodgkin's lymphoma (NHL). However, chemotherapy- and rituximab-refractory NHL patients may benefit from a regimen in which rituximab acts as a sensitizing agent. This study examined the apoptotic signaling mediated by rituximab on rituximab- and paclitaxel-resistant CD20$^+$ NHL B cell lines (Ramos, Raji, Daudi, and 2F7). Treatment with either rituximab (20 μg/ml) or paclitaxel (0.1–1000 nM) inhibited viable cell recovery of NHL lines. Neither rituximab nor paclitaxel induced significant apoptosis, although the combination treatment resulted in synergy in apoptosis. Rituximab selectively down-regulated Bcl-xL and induced apoptosis protease activating factor 1 (Apaf-1) expressions in Ramos cells. Paclitaxel down-regulated the expression of Bcl-xL and inhibitor of apoptosis proteins (c-IAP-1) and up-regulated the expression of Bad and Apaf-1. The combination treatment resulted in the formation of truncated Bid, cytosolic accumulation of cytochrome *c* and second mitochondria-derived activator of caspase/direct inhibitor of apoptosis-binding protein with low PI, activation of caspase-9, caspase-7, caspase-3, and cleavage of poly (ADP-ribose) polymerase. The findings identify two potential novel intracellular targets of rituximab-mediated signaling in Ramos NHL cells (*i.e.*, Bcl-xL and Apaf-1). Further, the findings show that both rituximab and paclitaxel selectively modify the expression pattern of proteins involved in the apoptosis signal transduction pathway and, through functional complementation, the combination results in synergy in apoptosis. The potential therapeutic significance of these findings is discussed. (Mol Cancer Ther. 2003;2:1183–1193)

Received 5/15/03; revised 7/23/03; accepted 8/24/03.

The costs of publication of this article were defrayed in part by the payment of page charges. This article must therefore be hereby marked advertisement in accordance with 18 U.S.C. Section 1734 solely to indicate this fact.

Grant support: Supported in part by the Boiron Research Foundation and a grant from the Department of Defense (U.S. Army DAMD 170210023). Ali Jazirehi was supported in part by a fellowship from the School of Dentistry and the Jonsson Comprehensive Cancer Center at UCLA.

Requests for Reprints: Benjamin Bonavida, Department of Microbiology, Immunology and Molecular Genetics, UCLA School of Medicine, A2-060 CHS, 10833 Le Conte Avenue, Los Angeles, CA 90095-1747.
Phone: (310) 825-2233; Fax: (310) 206-3865.
E-mail: bbonavida@mednet.ucla.edu

Introduction

Non-Hodgkin's lymphoma (NHL) is a heterogeneous group of disorders that represents about 4% of all malignancies and ranks fifth in cancer incidence and mortality (1, 2). Although the initial response rates to chemotherapy are high, relapse eventually occurs and subsequent chemotherapy regimens are incapable of yielding long-term remission (3). Failure of chemotherapy to eliminate tumor cells has prompted the development of alternative therapies. A novel treatment strategy is the use of antibody (Ab)-mediated immunotherapy alone or in combination with chemotherapy.

One of the candidate antigens that has been targeted for immunotherapy is CD20, a 297-amino acid (32–37 kDa) unglycosylated phosphoprotein that spans the membrane four times (4). Although the exact function of CD20 is not yet known, it is thought to play a role in the proliferation and differentiation of B lymphocytes (4). Approximately 80–85% of NHL are B-cell malignancies in origin and >95% of these express surface CD20. CD20 is exclusively expressed in the B-cell lineage, with minimal expression on early pre-B cells and normal plasma cells. It is neither shed from the cell surface nor modulated or internalized on Ab binding (5).

The anti-CD20 monoclonal Ab (mAb) rituximab (Rituxan, IDEC-C2B8) is the first mAb approved for therapeutic use in malignancies (6). Rituximab is active as a single agent in previously treated patients with various types of lymphomas with highly favorable toxicity profile (7–9). The mechanism of action of rituximab on CD20 ligation has not been clearly delineated; however, the involvement of Ab-dependent cellular cytotoxicity and complement-dependent cytotoxicity of the malignant cells has been suggested (6, 10). Rituximab exerts considerable cytotoxicity against malignant B cells when it is hyper-cross-linked, homodimerized, or used in combination with Fc receptor-expressing accessory cells, which mimics the *in vivo* microenvironment (5, 11, 12). Rituximab also exerts a cytostatic effect on NHL cell lines *in vitro* without induction of significant apoptosis (13–15).

The naturally occurring drug paclitaxel (Taxol) is effective in the treatment of drug-refractory bladder, prostate, ovarian, and metastatic breast carcinoma and leukemia (16). In addition to the effects on microtubules and cell cycle traverse, paclitaxel can cause significant cell killing by the induction of apoptosis and necrosis depending on the cell type and concentration used (17). There is accumulating evidence that paclitaxel, either alone or in combination with other drugs such as ifosfamide, 2-chlorodeoxadenosine, or high-dose cyclophosphamide, can be used in the treatment of patients with relapsed or refractory NHL (18).

We have shown that rituximab sensitizes the 2F7 NHL cells to chemotherapeutic drugs via down-regulation of Bcl-2 (19). Paclitaxel can induce Bcl-2 phosphorylation at serine residues 70 and 87, and this has been postulated to negatively regulate the antiapoptotic effects of Bcl-2 (20). Considering that the moderate effectiveness of rituximab and paclitaxel as single agents in modulating Bcl-2 levels is well established and the fact that most NHL cells overexpress Bcl-2, we hypothesized that the combination treatment of NHL cell lines with paclitaxel and rituximab may enhance the sensitivity of these cells to cytotoxic drugs and lead to synergistic apoptosis. Noteworthy, there are no studies on the combined effects of paclitaxel and rituximab in NHL. The objectives of the present study were (1) to investigate rituximab-mediated effects on the apoptotic signaling pathway, (2) to determine whether rituximab can be used as a sensitizing agent to enhance the cytotoxic activity of paclitaxel against paclitaxel-refractory NHL cell lines, (3) to delineate the modifications of the expression pattern of gene products associated with apoptosis that are induced by each agent, and (4) to establish whether the observed synergy in apoptosis by the combination treatment correlates with complementation in gene modification by each agent.

Materials and Methods

Cell Lines and Peripheral Blood Mononuclear Cells

The Burkitt's lymphoma B cell line 2F7 (also available via American Type Culture Collection, Bethesda, MD) was isolated from a single clone of a lymph node biopsy from a patient suffering from AIDS and were provided by Dr. Otoniel Martinez-Maza (UCLA, Los Angeles, CA). The human lymphoma B cell lines Ramos (21), Raji, and Daudi were purchased from the American Type Culture Collection. The tumor cell lines were maintained in sterile 75 cm^2 tissue culture flasks in RPMI 1640 (Life Technologies, Inc., Bethesda, MD) as described previously (19). The cell lines were maintained at a density of 0.5×10^6 cells/ml and were subcultured every 2 days.

For the generation of peripheral blood mononuclear cells (PBMC), whole blood from healthy donors was collected into 35 ml syringes with 0.5-ml sterile heparin. PBMCs were isolated by density centrifugation over a Ficoll-Hypaque density gradient (LSM, Durham, NC), washed thrice in sterile PBS, and immediately used in cytotoxicity assays.

Reagents

A stock solution of 10 mg/ml of rituximab was kept at 4°C and dilutions were prepared fresh for each experiment. Paclitaxel was dissolved in DMSO (Sigma Chemical Co., St. Louis, MO) to make a stock solution of 6 mg/ml and was kept at room temperature. For each experiment, paclitaxel was diluted by medium to obtain the indicated concentrations. The DMSO concentration did not exceed 0.1% in any experiment. Rituximab and paclitaxel were commercially acquired.

Mouse anti-Bcl-xL mAb was purchased from Santa Cruz Biotechnology (Santa Cruz, CA). Rabbit anti-Bad, anti-Bid, anti-caspase-9, anti-caspase-8, and anti-caspase-7 polyclonal Abs were purchased from Cell Signaling (Beverly, MA). Mouse anti-procaspase-3 and FITC-labeled anti-active caspase-3 mAbs were obtained from PharMingen (San Diego, CA). Mouse anti-actin mAb and rabbit anti-apoptosis protease activating factor 1 (Apaf-1) polyclonal Abs were purchased from Chemicon International, Inc. (Temecula, CA). Rabbit anti-survivin polyclonal Ab was purchased from Proscience Inc. (Poway, CA). Rabbit anti-inhibitors of apoptosis proteins (c-IAP-1 and c-IAP-2) and X-chromosome-linked inhibitor of apoptosis (XIAP) polyclonal Abs were purchased from Trevegen, Inc. (Gaithersburg, MD). Mouse anti-cytochrome *c* mAb and rat anti-second mitochondria-derived activator of caspase/direct inhibitor of apoptosis-binding protein with low pI (Smac/DIABLO) polyclonal Ab were purchased from PharMingen and Alexis Biochemicals (San Diego, CA), respectively. The Bcl-xL inhibitor 2-methoxyantimycin A3 (2MAM-A3) was purchased from Biomol (Plymouth, PA).

Rituximab Pretreatment

Ramos and 2F7 tumor cell lines (10^6 cells/ml) were grown in complete medium in 10 cm^2 tissue culture dishes (Life Technologies, Inc., Gaithersburg, MD) and were treated with a previously established optimal concentration (20 μg/ml) of rituximab for 48 h (15, 22). The cells were then washed and fresh medium was added and seeded into six-well plates (Costar, Cambridge, MA). Indicated concentrations of paclitaxel were then added, and the cells were incubated for another 16 h for maximal cytotoxicity. At the end of the incubation period, the cells were harvested and subjected to propidium iodide (PI) staining according to the specifications of the PI staining kit (Roche Diagnostics Corporation, Indianapolis, IN) and evaluated by flow cytometric analysis.

Cell Cycle Distribution and Assessment of Apoptosis by Flow Cytometric Analysis

The percentage of apoptotic cells was determined by evaluation of PI-stained preparations as described previously (5, 23) and by caspase activity (see below) of paclitaxel/rituximab-treated tumor cell lines. Cell cycle analysis and apoptosis were determined using an EpicXL flow cytometer. A minimum of 6000 events was collected on each sample and acquired in listmode by a PC Pentium computer. Cellular debris was excluded from analysis by raising the forward scatter threshold, and the DNA content

of the intact nuclei was recorded on a logarithmic scale (5, 23). The percentage of apoptotic cells is represented as the percentage of hypodiploid cells accumulated at the sub-G_0 phase of the cell cycle.

Caspase-3 Activity Measured by Flow Cytometric Analysis

Ramos cells (10^6 cells/ml) were grown in complete medium (control) or treated with rituximab (20 μg/ml, 48 h), paclitaxel (10 nM, 16 h), or combination of rituximab and paclitaxel. At the end of the incubation period, cells were washed once with ice-cold 1× PBS/0.1% BSA and were resuspended in 100-μl ice-cold 1× PBS/0.1% BSA. 50 μl of cell suspension (containing 2×10^6 cells) were aliquoted to each sample and were fixed with Cytofix/Cytoperm solution (PharMingen) for 20 min. Thereafter, the samples were washed twice with ice-cold 1× Perm/Wash buffer solution (PharMingen) and were stained with FITC-labeled anti-active caspase-3 mAb for 30 min (light protected). Thereafter, the samples were washed once with ice-cold 1× PBS/0.1% BSA followed by flow cytometric analysis. As negative control, the cells were stained with isotype control (pure IgG1) under the same conditions described above.

Cell Viability as Measured by Trypan Blue Dye Exclusion Assay

The Ramos and 2F7 cells were cultured in complete medium (control) or complete medium supplemented with rituximab, paclitaxel, and rituximab/paclitaxel under the same conditions explained above. At the end of the incubation period, the cells were harvested, a small aliquot of the cell suspension was removed and mixed with an equal volume of 0.4% trypan blue dye solution, and cell viability was determined by light microscopy. The results are representative of mean ± SD of calculated viable and dead cell numbers from three independent experiments.

Analysis of Mitochondrial Membrane Potential by 3,3′-Dihexyloxacarbocyanine Iodide Staining

Ramos cells were stained with 3,3′-dihexyloxacarbocyanine iodide [$DiOC_6(3)$] to quantitate mitochondrial membrane potential. The cells were analyzed by flow cytometry with an EpicXL flow cytometer as described previously (24).

Western Blot Analysis

Tumor cells (10^7 cells/treatment) were left either untreated (control) or treated with rituximab (20 μg/ml, 48 h) or paclitaxel (10 nM, 16 h) or pretreated with rituximab (20 μg/ml, 48 h) followed by paclitaxel (10 nM, 16 h) treatment. The cells were then lysed at 4°C in radioimmunoprecipitation assay buffer as described previously (25). The cell lysates (40 μg) were then electrophoresed on 12% SDS-PAGE gels (Bio-Rad, Hercules, CA) and were subjected to Western blot analysis (25). Levels of β-actin were confirmed to ensure equal loading of the samples. The relative intensity of the bands was assessed by densitometric analysis of the digitized images and performed on an iMac computer (Apple Computer Inc., Cupertino, CA) using the public domain NIH image program (developed at NIH and also available on the Internet at http://rsb.info.nih.gov/nih-image/). Alterations of ≥40% were considered significant.

Isolation of Cytosolic Fraction and Determination of Cytochrome *c* and Smac/DIABLO Content

Ramos cells (10^7 cells/treatment) were grown under the conditions explained for Western blot. At the end of the incubation period, cells were washed twice with 1-ml ice-cold 1× PBS/0.1% BSA and were resuspended in 2 volumes of homogenization buffer (20-mM HEPES [pH 7.4], 10-mM KCl, 1.5-mM $MgCl_2$, 1-mM sodium EDTA, 1-mM sodium EGTA, 1-mM DTT, one tablet of Complete Mini protease inhibitor cocktail in 250-mM sucrose medium). After 30 min on ice, the cells were disrupted by 40 strokes of a Dounce glass homogenizer using a loose pestle (Bellco Glass, Inc., Vineland, NJ). The homogenate was centrifuged at 2500×*g* at 4°C for 5 min to remove nuclei and unbroken cells. The mitochondria were pelleted by spinning the homogenate at 16,000×*g* at 4°C for 30 min. The supernatant was removed and filtered through 0.1 μm Ultrafree MC filters (Millipore, Billerica, MA) to obtain the cytosolic fraction and was spun down at 16,000×*g* at 4°C for 15 min. The protein concentration of the supernatant was determined by the DC assay kit and was mixed with 2× Laemelli sample buffer and analyzed by SDS-PAGE for determination of cytochrome *c* and Smac/DIABLO contents in the cytosolic fraction.

Isobolographic Analysis for Determination of Synergy

Determination of the synergistic *versus* additive *versus* antagonistic cytotoxic effects of the combination treatment of the Ramos and 2F7 cell lines by rituximab and paclitaxel was assessed by isobolographic analysis as described previously (26). Briefly, isobolograms were constructed from a battery of combinations of various concentrations of rituximab (1, 10, 20, 50, 75, and 100 μg/ml) with paclitaxel (0.1–1000 nM). Combinations yielding 30 ± 5% cytotoxicity were plotted as percentage of single agent alone that resulted in the same percentage of cytotoxicity (fractional inhibitory concentration: concentration of each agent in combination/concentration of each agent alone). When the sum of this fraction (fractional inhibitory concentration) is 1, the combination is additive and the graph is geometrically expressed as a straight line; when the sum is <1, the combination is synergistic and the graph appears as concave shape; and when the sum is >1, the combination is antagonistic and the graph is geometrically represented as convex shape.

Statistical Analysis

Assays were set up in triplicates and the results were expressed as the mean ± SD. Statistical analysis and *P* value determinations were done by two-tailed paired *t* test with a confidence interval of 95% for determination of the significance of differences between the treatment groups. $P < 0.05$ was considered to be significant. ANOVA was used to test the significance among the groups. The InStat 2.01 software was used for analysis.

Results

Inhibition of Ramos and 2F7 Viable Cell Recovery by Rituximab and Paclitaxel

Flow cytometry data showed that the majority of the Ramos and 2F7 cells (>95%) express CD20 (data not shown).

Significant inhibition of viable cell recovery was observed in both cell lines on treatment with rituximab and a plateau was reached at rituximab concentrations of ≥20 μg/ml. Maximum inhibition of cell recovery was 32% for Ramos and 51% for 2F7 (Fig. 1A). The inhibition of cell recovery was not due to cytotoxicity as <7% of the cells were dead at 48 h of incubation (Table 1). Rituximab also inhibited cell recovery of Daudi (43%) and Raji (24%) NHL B cell lines (data not shown). Paclitaxel exerted inhibition of viable cell recovery and a plateau of ~60% of inhibition was achieved for Ramos at paclitaxel concentrations of ≥100 nM. For 2F7, the inhibition was more pronounced and as much as 36% inhibition was obtained at paclitaxel concentrations of ≥1 nM (Fig. 1B). The inhibitory effect of the combination treatment of rituximab and paclitaxel was also examined. There was no additional inhibition above that achieved by paclitaxel alone (Fig. 1C). These findings demonstrate that both rituximab and paclitaxel, alone or in combination, inhibited viable cell recovery of NHL B cell lines.

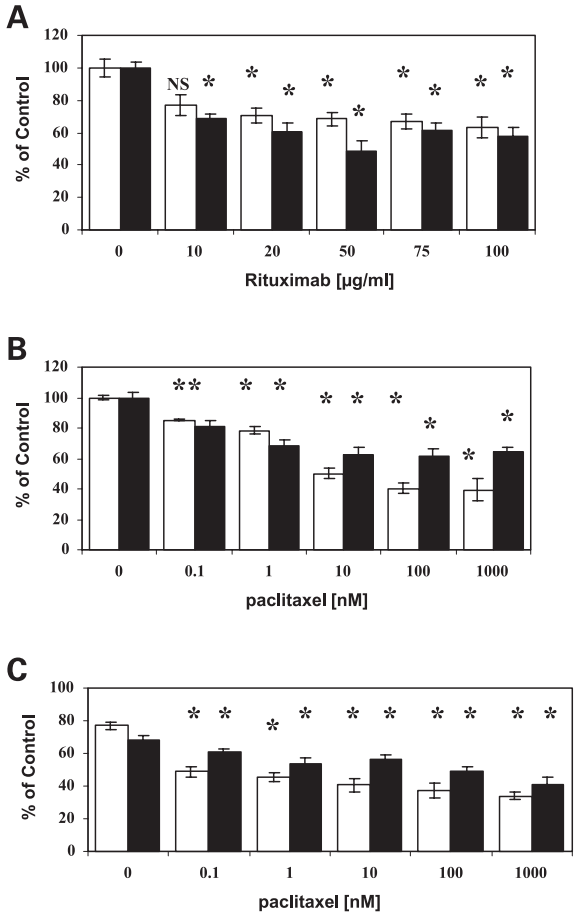

Figure 1. Cytostatic effects of rituximab, paclitaxel, and rituximab + paclitaxel on Ramos (□) and 2F7 (■) cell lines. Cells were either left untreated or treated with various concentrations of (**A**) rituximab (0 – 100 μg/ml, 48 h), (**B**) paclitaxel (0.1 – 1000 nM, 16 h), (**C**) or rituximab (20 μg/ml, 48 h) + paclitaxel (0.1 – 1000 nM, 16 h). At the end of the incubation period, the percentage of inhibition of viable cell recovery was measured microscopically by the trypan blue dye exclusion method. *Columns,* mean; *bars,* SD (n = 3). *, P < 0.01 (significant) compared with control.

Effects of Rituximab, Paclitaxel, and Combination on Cell Cycle

Rituximab and paclitaxel, alone and in combination, were evaluated for their effects on the cell cycle distribution. The findings are summarized in Fig. 2 and Table 1. The Ramos and 2F7 cells were treated with rituximab (20 μg/ml, 48 h) and paclitaxel (1 and 10 nM, 16 h). The results of three independent experiments demonstrate that rituximab has no effect on the cell cycle distribution of Ramos and 2F7 cells. Paclitaxel induced significant arrest of both cell lines at the G_2-M phase of the cell cycle and the extent of cell cycle arrest inversely correlated with the paclitaxel concentration used. The combination treatment-pretreatment with rituximab for 48 h followed by paclitaxel for 16 h showed less cells arrested at G_2-M.

Synergy Is Achieved for Apoptosis by Combination Treatment of Ramos Cells with Paclitaxel and Rituximab

We examined whether the sensitizing effect of rituximab to paclitaxel-mediated cytotoxicity was synergistic (26). Flow cytometric analysis, as illustrated in Fig. 2A, clearly demonstrates that rituximab treatment alone does not induce apoptosis in Ramos cells. Paclitaxel, however, induced moderate apoptosis at 1 nM, which was not potentiated by 10-fold increase (Table 1; Fig. 2A). In contrast, the combination of rituximab (20 μg/ml) and paclitaxel (1 nM, 10 nM) resulted in significant potentiation of apoptosis as shown by the accumulation of the hypodiploid cells at the sub-G_0 phase of the cell cycle (Fig. 3A; Table 1). At the 1 and 10 nM concentrations of paclitaxel, >35% and >43% of the cells underwent apoptosis, respectively. A representative experiment is depicted in Fig. 2A and the mean of three experiments is shown in Table 1. The observed augmentation of apoptosis by the combination treatment with rituximab and paclitaxel resulted in synergistic apoptosis as determined by isobolographic analysis (Fig. 3). Time kinetics studies demonstrated that induction of apoptosis by the combination treatment started at 8–12 h post-treatment and reached the maximum levels by 16 h. Prolongation of the incubation period did not enhance the level of apoptosis (data not shown).

To validate the PI staining and sub-G_0 hypodiploid cell population as the true representatives of apoptosis (5, 23), the Ramos cells were treated under the conditions mentioned above. The samples were divided into two equal proportions. One proportion was subjected to PI staining and DNA fragmentation analysis and the other half was stained with FITC-labeled anti-active caspase-3 mAb. A close correlation was established between the percentage of hypodiploid cells accumulating at the sub-G_0 region with those possessing active caspase-3 (Table 2). Collectively, these results validate the DNA fragmentation assay (PI) for the measurement of apoptosis.

Under the same conditions, 2F7 cells were examined for synergy by the combination treatment. No synergy in apoptosis was achieved by the combination of rituximab and paclitaxel (Fig. 3B). The failure to detect sensitization by rituximab to paclitaxel-mediated apoptosis (Fig. 2B) was

Table 1. Cell cycle analysis and apoptosis by rituximab, paclitaxel, and combination treatment of Ramos and 2F7 NHL cell lines

Treatment	G_0-G_1	S	G_2-M	Apoptosis
Ramos				
Control	42.0 ± 6.2	25.7 ± 2.9	27.1 ± 3.8	3.8 ± 0.7
DMSO	38.3 ± 3.7	28.1 ± 4.1	26.1 ± 6.5	6.0 ± 2.2
Rituximab (20 μg/ml)	37.5 ± 5.1	28.0 ± 4.1	30.3 ± 5.2	2.7 ± 0.6
Paclitaxel (1 nM)	16.8 ± 0.4	9.2 ± 1.3	60 ± 1.5	13.3 ± 1.8
Paclitaxel (10 nM)	26.4 ± 2.8	20.1 ± 8.5	39.9 ± 6	12.4 ± 0.8
Rituximab (20 μg/ml) + paclitaxel (1 nM)	24.3 ± 4.1	19.3 ± 0.9	22.5 ± 0.7	35.5 ± 5.1[a]
Rituximab (20 μg/ml) + paclitaxel (10 nM)	19.6 ± 3.2	16.3 ± 3.9	21.4 ± 2.9	45.3 ± 2.5[a]
2F7				
Control	48.8 ± 6.3	20.4 ± 1.1	23.5 ± 6.0	6.5 ± 1.7
DMSO	49.4 ± 1.4	20.1 ± 0.5	22.5 ± 2	7.2 ± 1.5
Rituximab (20 μg/ml)	54.6 ± 1.6	18.6 ± 0.6	18.1 ± 1.8	7.9 ± 0.6
Paclitaxel (1 nM)	22.1 ± 2.2	9.8 ± 2.2	46 ± 1.9	21.2 ± 2.4
Paclitaxel (10 nM)	18.1 ± 1.6	14.4 ± 3.2	48.1 ± 3.8	18.7 ± 1.9
Rituximab (20 μg/ml) + paclitaxel (1 nM)	23.7 ± 3.6	7.5 ± 2.2	46.2 ± 3.8	22.3 ± 2.4[b]
Rituximab (20 μg/ml) + paclitaxel (10 nM)	29.8 ± 7.3	15.2 ± 4.9	42.9 ± 1	10.8 ± 1.3[b]

Note: The cells (Ramos and 2F7) were either left untreated (control) or pretreated with rituximab (20 μg/ml, 48 h). Thereafter, the cells were washed, fresh medium was added, and the cells were incubated with various concentrations of paclitaxel (1 and 10 nM, 16 h). At the end of the incubation period, the cells were stained with PI solution and cell cycle analysis was assessed by flow cytometry. The percent apoptosis was determined as the percentage of hypodiploid cells accumulated at the sub-G_0 phase of the cell cycle. The results are represented as mean ± SD (n = 3).

[a] $P < 0.001$ (very significant).

[b] Not significant compared with paclitaxel treatment alone.

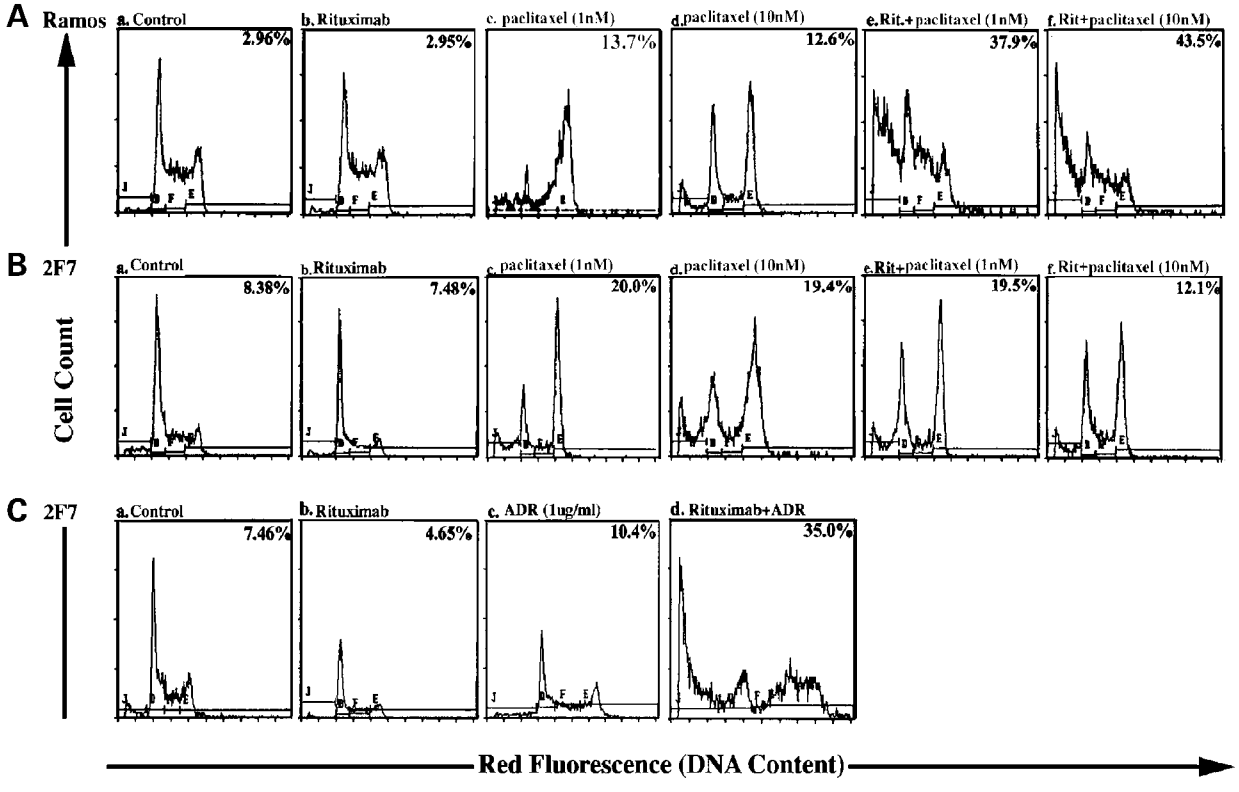

Figure 2. Sensitization of Ramos and 2F7 cell lines by rituximab to paclitaxel and ADR-mediated apoptosis. Ramos and 2F7 cells were either left untreated or pretreated with rituximab (20 μg/ml, 48 h). Thereafter, the cells were washed, fresh medium was added, and the cells were incubated with various concentrations of (**A** and **B**) paclitaxel (1 and 10 nM, 16 h) or (**C**) ADR (1 μg/ml) was added to the rituximab-pretreated 2F7 cells for an additional 16 h. Then, the cells were stained with PI solution (DNA fragmentation assay) and analyzed by flow cytometry. The percentage of apoptotic cells (sub-G_0 population) is indicated at the upper right corner of each panel. The findings demonstrate that rituximab sensitizes Ramos and not 2F7 to paclitaxel-mediated apoptosis. However, rituximab sensitizes 2F7 to ADR-mediated apoptosis. The results are representative of three independent experiments.

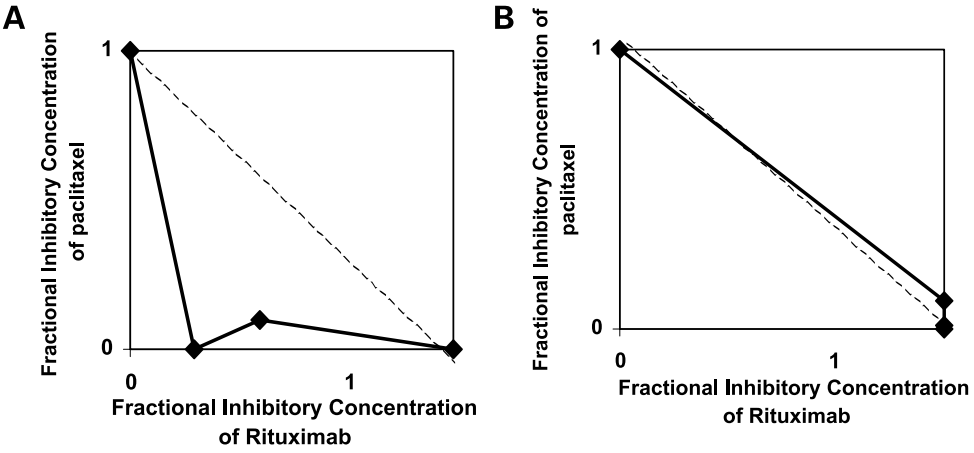

Figure 3. Isobolographic analysis for the determination of synergistic effects of rituximab/paclitaxel combination treatment on Ramos (**A**) and 2F7 (**B**) cell lines. The cells were treated under the conditions explained in Fig. 2, and the synergistic *versus* additive *versus* antagonistic effects of rituximab/paclitaxel treatment of both cell lines was evaluated by isobolographic analysis as described previously (26). Synergy is shown for Ramos and not for 2F7 cells.

not due to the inherent resistance of 2F7 cells to the sensitizing effects of rituximab. Treatment of the 2F7 cells with rituximab sensitized the cells to Adriamycin (ADR)-induced apoptosis (Fig. 2C).

Rituximab-mediated sensitization to paclitaxel-induced apoptosis was not limited to the Ramos cells. Pretreatment of other NHL cells such as Raji and Daudi with rituximab rendered them sensitive to apoptosis induced by paclitaxel (Table 3). Noteworthy, the combination of rituximab and paclitaxel was not toxic and did not potentiate the killing of freshly derived human PBMCs beyond the background levels (Fig. 4). At 10 nM paclitaxel, rituximab-pretreated PBMCs exhibited 9 ± 1.6% apoptosis compared with rituximab (6.0 ± 1.8%) or paclitaxel (5.9 ± 1.1%) treatment alone.

The above data demonstrate that rituximab is capable of sensitizing paclitaxel-resistant NHL B cell lines to paclitaxel-induced apoptosis, whereas minimal toxicity is observed by the combination on PBMC.

Effects of Rituximab and Paclitaxel, Alone and in Combination, on the Expression of Apoptotic Regulatory Proteins in Ramos Cells

We have chosen Ramos cells as the model to examine the mechanism of sensitization by rituximab to paclitaxel mediated apoptosis. We have postulated that signaling may result from alterations in the expression levels of a number of proapoptotic as well as antiapoptotic gene products on rituximab and paclitaxel treatments. Rituximab treatment of Ramos cells resulted in down-regulation of Bcl-xL expression and up-regulation of Apaf-1. Rituximab did not regulate the expression of several other apoptotic gene products examined (Fig. 5, A and E). Treament of Ramos cells with paclitaxel resulted in down-regulation of the antiapoptotic proteins Bcl-xL and c-IAP-1. Paclitaxel up-regulated the expression of proapoptotic Bad and significantly induced Apaf-1 expression (Fig. 5, A and E). Combination of rituximab and paclitaxel resulted in complete abrogation of Bcl-xL expression and pronounced decrease in the expression of survivin, c-IAP-1, and c-IAP-2. However, the expression level of XIAP was not significantly altered by the combination treatment (Fig. 5, A and D). In addition, the combination treatment resulted in the cleavage of Bid (truncated Bid [tBid]), another proapoptotic member of the Bcl-2 family, which migrates to the mitochondria and ensures mitochondrial destabilization.

Neither rituximab nor paclitaxel significantly activated caspase-3, caspase-7, or caspase-9 (Table 2; Fig. 5B). These caspases were activated by the combination treatment, leading to the cleavage of poly(ADP-ribose) polymerase (PARP) (Fig. 5B). The instability of mitochondria was further enhanced by significant decrease in mitochondrial transmembrane potential ($\Delta\psi m$) by the combination of

Table 2. Comparison of apoptosis measured by PI staining and caspase-3 activation

	% Apoptosis			
	Control	Rituximab (20 μg/ml)	Paclitaxel (10 nM)	Rituximab + paclitaxel
PI staining	1.32 ± 0.26	1.85 ± 0.8	12.08 ± 1.4	46.9 ± 1.9
Caspase-3 activation	5.34 ± 1.82	9.7 ± 2.8	10.9 ± 12.2	46.7 ± 3.3

Note: The Ramos cells were treated under the same conditions explained in Table 1. Thereafter, the samples were divided in two equal proportions. One half was subjected to PI staining and the percent apoptosis was measured by the percent of hypodiploid cells accumulated at sub-G_0 phase of the cell cycle. The second half was subjected to staining with FITC-labeled anti-active caspase-3 mAb and fluorescence-activated cell sorting analysis. Samples were set up in duplicates and the results are represented as means ± SEM (n = 2).

paclitaxel and rituximab (Table 4; Fig. 5D). Further analysis revealed significant accumulation of cytochrome *c* and Smac/DIABLO in the cytosolic fraction (Fig. 5, C and E) by the combination treatment. Cytosolic accumulation of these proteins paralleled their depletion from mitochondrial fraction (data not shown), which confirms their redistribution from the mitochondria to the cytosol.

Collectively, these results demonstrate that rituximab and paclitaxel selectively inhibit the expression of Bcl-xL and up-regulate the expression of Apaf-1 in Ramos cells. In addition, paclitaxel up-regulates Bid and inhibits c-IAP-1 expression. Further, the findings demonstrate that each agent, by itself, was insufficient for the full activation of the mitochondrial pathway for apoptosis. However, the combination of rituximab and paclitaxel, by functional complementation, activated the mitochondrial pathway and facilitated the apoptotic signal to fully proceed toward apoptosis.

Role of Bcl-xL Expression in Resistance to Paclitaxel-Induced Apoptosis

The above findings demonstrate that rituximab selectively down-regulates the expression of antiapoptotic Bcl-xL in Ramos cells, which might be implicated as pivotal to maintain resistance to paclitaxel. Accordingly, inhibition of Bcl-xL activity should mimic rituximab effects and sensitize the cells to paclitaxel-induced apoptosis. This was tested by the use of a specific inhibitor. 2MAM-A3 has protein binding activity and binds to the hydrophobic groove bounded by the BH1, BH2, and BH3 domains on the surface of Bcl-xL (27), thus preventing its dimerization with the proapoptotic Bcl-2 family members. This will alter the proapoptotic/antiapoptotic ratio and favor the apoptotic signaling to proceed.

To ascertain the protective role of Bcl-xL in Bcl-2-deficient Ramos cells, the cells were either left untreated or pretreated with rituximab (20 μg/ml, 48 h) or 2MAM-A3 (15 μg/ml, 6 h). Thereafter, the cells were washed, fresh medium was added, and the cells were incubated with paclitaxel (10 nM, 16 h). At the end of the incubation period, the cells were subjected to PI staining (DNA fragmentation assay) and flow cytometric analysis. 2MAM-A3 induced modest apoptosis in Ramos cells (9.1 ± 1.5%). However, it sensitized the cells to paclitaxel-induced apoptosis at levels comparable with that achieved by rituximab pretreatment (37.1 ± 1.8%; $P < 0.05$, compared with paclitaxel alone). Similar results were obtained with other cell lines (data not shown). These findings suggest that diminished expression (by rituximab) and functional impairment (by 2MAM-A3) of Bcl-xL is sufficient to overcome paclitaxel resistance.

Table 3. Rituximab-mediated sensitization of NHL cell lines to paclitaxel-induced apoptosis

	Paclitaxel (nM)			
	Control	0.1	1	10
Raji	3.0 ± 2.8	6.5 ± 1.1	17.7 ± 2.1	19.8 ± 1.6
Raji + rituximab	4.8 ± 1.2	12.2 ± 1.3[a]	28.8 ± 1.6[b]	31.2 ± 1.5[b]
Daudi	2.4 ± 1.1	3.8 ± 2.1	6.3 ± 0.7	11.6 ± 1.4
Daudi + rituximab	5.9 ± 3.2	13.3 ± 1.9[b]	18.7 ± 1.6[c]	23.5 ± 1.7[b]

Note: Raji and Daudi cells were treated under the conditions explained in Table 1 and the percentage of apoptosis was determined by flow cytometry. Samples were set up in duplicates and the data are represented as means ± SD ($n = 2$).
[a]Not significant compared with paclitaxel treatment alone.
[b]$P < 0.01$ (significant).
[c]$P < 0.001$ (very significant).

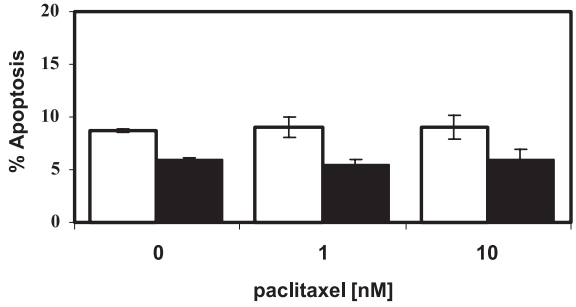

Figure 4. Failure of rituximab to sensitize PBMCs to paclitaxel-mediated apoptosis. PBMCs (10^6 cells/ml) were either left untreated (□) or pretreated with rituximab (■; 20 μg/ml, 48 h). Thereafter, the cells were washed, fresh medium was added, and the cells were incubated with various concentrations of paclitaxel (1 and 10 nM, 16 h). Then, the cells were stained with PI solution (DNA fragmentation assay) and analyzed by flow cytometry. *Columns,* mean; *bars,* SD ($n = 2$). The data show that the combination treatment was not toxic to PBMC.

Discussion

The present study provides evidence for the first time that treatment of refractory NHL cell lines with rituximab potentiates the cytotoxic effect of paclitaxel and leads to synergy in apoptosis. The observed synergy in apoptosis achieved by the combination of rituximab and paclitaxel appears to be the result of complementation by the selective modification of apoptosis regulatory proteins by each agent alone. Rituximab selectively down-regulated the expression of antiapoptotic Bcl-xL and up-regulated the expression of proapoptotic Apaf-1 in Ramos cells. These modifications along with those exerted by paclitaxel were presumably sufficient to avert the resistance to apoptosis of paclitaxel-refractory NHL cells. Hence, the combination treatment resulted in the destabilization of the mitochondria, release of cytochrome *c* and Smac/DIABLO, activation of caspase-3, caspase-7, and caspase-9, subsequent cleavage of caspase substrates, and apoptosis. These data demonstrate that the combination of rituximab and subtoxic concentrations of paclitaxel, both used at clinically achievable concentrations (16, 22), may be effectively used against paclitaxel-refractory NHL.

It is well documented that paclitaxel inhibits microtubule depolymerizarion and promotes the formation of metastable microtubules. This interferes with the normal function of microtubules, prevention of mitotic spindle formation, and subsequent arrest of the cell cycle progression at the late G_2-M phases (16). In agreement, paclitaxel caused G_2-M arrest of all of the four NHL B cell lines used in the study, albeit with varying degrees.

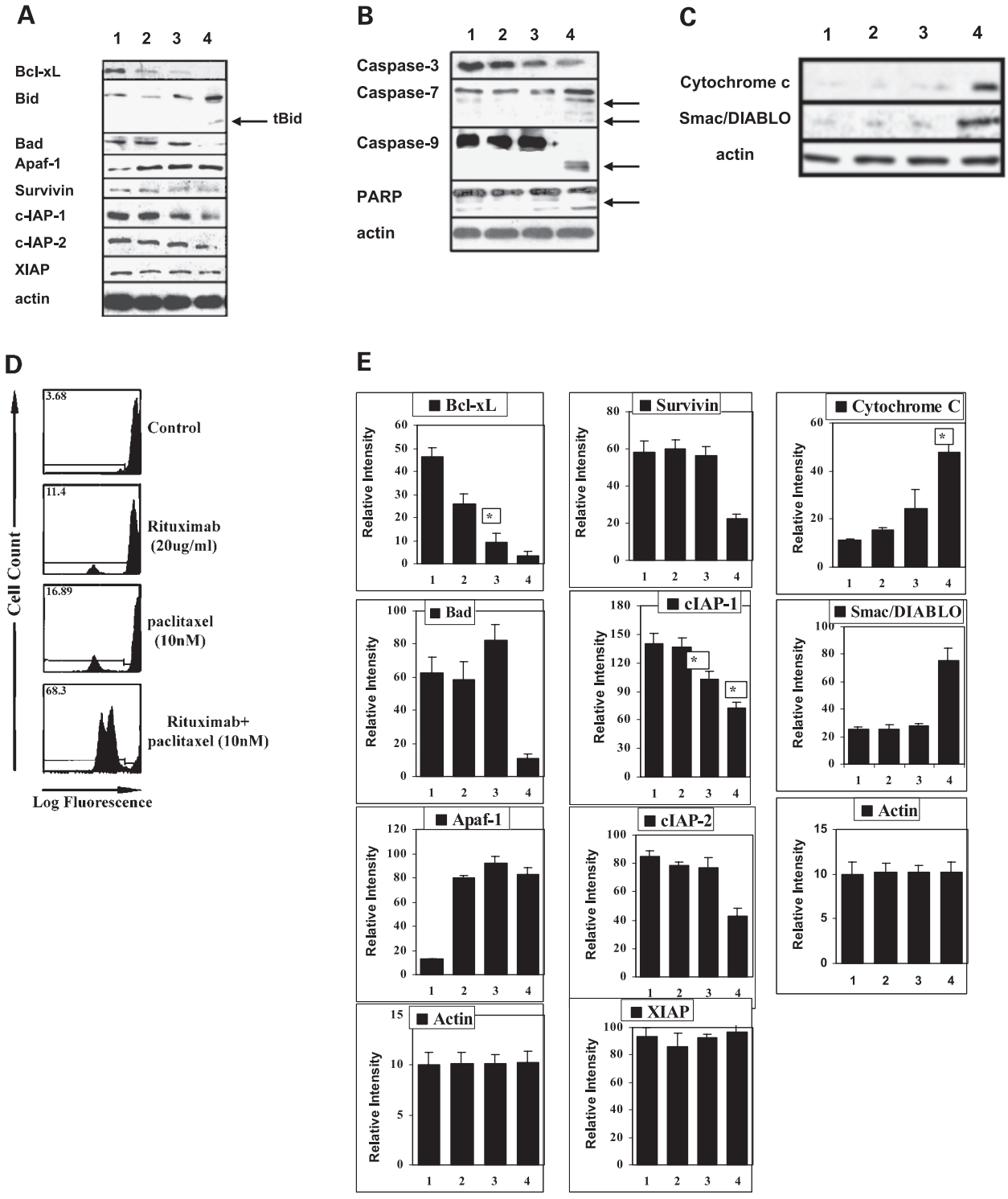

Figure 5. Western blot analysis for detection of alterations in protein expression by rituximab, paclitaxel, or combination. **A,** modifications of apoptotic gene products; **B,** activation of caspases and PARP cleavage; **C,** cytosolic accumulation of cytochrome *c* and Smac/DIABLO; **D,** flow cytometry histograms demonstrating alterations in $\Delta\psi_m$; **E,** densitometric analysis and the relative intensity of the modulation of apoptosis regulatory gene products. Ramos cells were grown in (*1*) the absence (complete medium control), (*2*) the presence of rituximab (20 μg/ml, 48 h), (*3*) the presence of paclitaxel (10 nM, 16 h), or (*4*) pretreatment with rituximab (20 μg/ml, 48 h) + paclitaxel (10 nM, 16 h). Total cell lysates [C: cytosolic fractions] (40 μg) were subjected to Western blot analysis as described in ''Materials and Methods.'' Relative intensity of the bands and statistical significance were assessed as described in ''Materials and Methods.'' Analysis of $\Delta\psi_m$ was performed as detailed in Table 4. *Arrows,* cleaved form of the proteins. *Columns,* mean; *bars,* SD ($n = 2$).

Table 4. Alterations in $\Delta\psi m$ by the combination of rituximab and paclitaxel

Control	% Alterations in $\Delta\psi m$		
	Rituximab (20 μg/ml)	Paclitaxel (10 nM)	Rituximab + paclitaxel
9.6 ± 2.8	11.7 ± 1.3	14.8 ± 2.9	53.8 ± 4.8

Note: The Ramos cells were treated under the same conditions explained in Table 1. After the incubation period, the cells were washed, stained with $DiOC_6(3)$ for 30 min at 37°C, and analyzed by flow cytometry. The samples were set up in duplicates and the results are presented as means ± SD of percentage of the cells with depolarized mitochondria (n = 2).

Rituximab treatment of NHL cells neither induced perturbations in cell cycle distribution nor induced significant cytotoxicity in NHL cell lines. In contrast to mouse anti-CD20 mAbs such as 1F5 that stimulates cell cycle transition from G_0 to G_1 or B1, which inhibits B-cell progression from G_1 to S-G_2-M phase of the cell cycle (4, 5), the antihuman CD20 mAb rituximab inhibits cellular proliferation with no apparent effects on any specific phase of the cell cycle (19). Rituximab alone does not induce apoptosis, whereas previous findings showed that hyper-cross-linking (11) or homodimers (12) of rituximab are capable of inducing apoptosis. The failure of rituximab to induce apoptosis in this study can be explained by the usage of monomeric (non-cross-linked) rituximab.

Rituximab pretreatment sensitized Ramos cells to paclitaxel-mediated apoptosis (Table 1; Fig. 2A) in a synergistic manner (Fig. 3A). Rituximab also sensitized additional NHL cell lines to paclitaxel-induced apoptosis (Table 3). In contrast, rituximab failed to sensitize the 2F7 cells to paclitaxel-induced apoptosis (Fig. 2B; Table 1). This failure is not due to an inherent inability of rituximab to sensitize the 2F7 cells to chemotherapeutic drugs because rituximab sensitized the 2F7 cells to apoptosis induced by ADR (Fig. 2C) and other drugs (15).

To delineate the potential underlying molecular mechanism of the observed synergy in apoptosis in Ramos cells, we present evidence that both rituximab and paclitaxel down-regulated the expression of Bcl-xL at the protein level (Fig. 5A). While we have previously demonstrated that rituximab down-regulates Bcl-2 in 2F7 (19), in this study, however, we demonstrate that in Bcl-2-deficient Ramos cells (11) the Bcl-2 homologue, Bcl-xL, is a novel intracellular target of rituximab. Rituximab-induced down-regulation of Bcl-xL was also noticed in other NHL B cell lines studied (Raji and Daudi; data not shown). The mechanism by which rituximab inhibits Bcl-xL is not known. Preliminary findings suggest that rituximab inhibits its activator protein-1 (AP-1) activity, which has been shown to regulate Bcl-xL expression (28). Paclitaxel also down-regulated Bcl-xL expression, which is in agreement with previously reported data (29). Accumulating evidence suggests a regulatory role of Bcl-xL in the paclitaxel signal transduction pathway. Bcl-xL-expressing ovarian carcinoma and hepatoblastoma HepG2 cells exhibited high resistance to paclitaxel and other drugs (30, 31). Ectopic overexpression of Bcl-xL blocks paclitaxel, etoposide, ADR, and camptothecin induced apoptosis in HL-60, NIH3T3 fibroblasts, and IL-3-dependent murine myeloid 32D cells (32). Our findings are in agreement with these results. Further, previous findings have shown that functional impairment of Bcl-xL in cells expressing high levels of Bcl-xL can overcome the drug resistance and induce apoptosis (27). Our findings suggest that decreased expression and functional impairment of Bcl-xL by rituximab (Fig. 5A) and 2MAM-A3, respectively, are sufficient to overcome paclitaxel resistance in Ramos NHL cells. Further, these findings suggest the role of Bcl-xL as a resistant factor and suggest that the inhibition of Bcl-xL expression by rituximab in Ramos cells is responsible for sensitization to paclitaxel-induced apoptosis.

Slight induction of Bad was observed on paclitaxel treatment of Ramos cells (Fig. 5A). Bad has been shown to partly account for paclitaxel resistance of ovarian carcinoma cells (33). Because the ratio between death repressors and death promoters of the Bcl-2 family members is a key determinant of the cellular fate in response to noxious stimuli, our results suggest that concurrent decrease in Bcl-xL and increase in Bad protein levels will favor the apoptosis signal to proceed.

Significant up-regulation of Apaf-1 expression by rituximab and paclitaxel was observed (Fig. 5A). Recently, we have reported that up-regulation of Apaf-1 by ADR might be implicated in the sensitization of ADR-resistant human multiple myeloma cells to tumor necrosis factor-related apoptosis-inducing ligand-induced apoptosis (25). Enforced overexpression of ectopic Apaf-1 decreased the threshold of apoptosis of HL-60 cells in response to etoposide and paclitaxel (24, 34), which was inhibited in cells with high levels of Bcl-2 or Bcl-xL (31). Rituximab, via direct or indirect DNA damage, in a p53-dependent manner (35), may up-regulate Apaf-1. Rituximab may also increase the protein stability of Apaf-1 via a proteosome-dependent pathway.

We have also observed slight down-regulation of c-IAP-1 by paclitaxel. IAP family members (c-IAP-1, c-IAP-2, XIAP, and survivin) selectively suppress different apoptotic pathways initiated by stimuli that release cytochrome *c* from mitochondria. IAPs inhibit these pathways through the binding to and ablating of the proteolytic processing of distinct caspases that function in the distal portions of the proteolytic cascades involved in apoptosis such as caspase-3, caspase-6, caspase-7, and caspase-9 but not the upstream initiator caspase-8 (36–38)

Combination of rituximab and paclitaxel resulted in total loss of Bcl-xL and pronounced down-regulation of survivin and both c-IAP-1 and c-IAP-2. IAP family members are expressed in a large panel of tumors from various origins including NHL while undetectable in normal adult tissues (36–38). Because most chemotherapeutic agents exert their effects via the mitochondrial pathway (type II) and the fact that IAPs do not bind to caspase-8, the expression of IAPs might reflect an additional level of protection of NHL cells

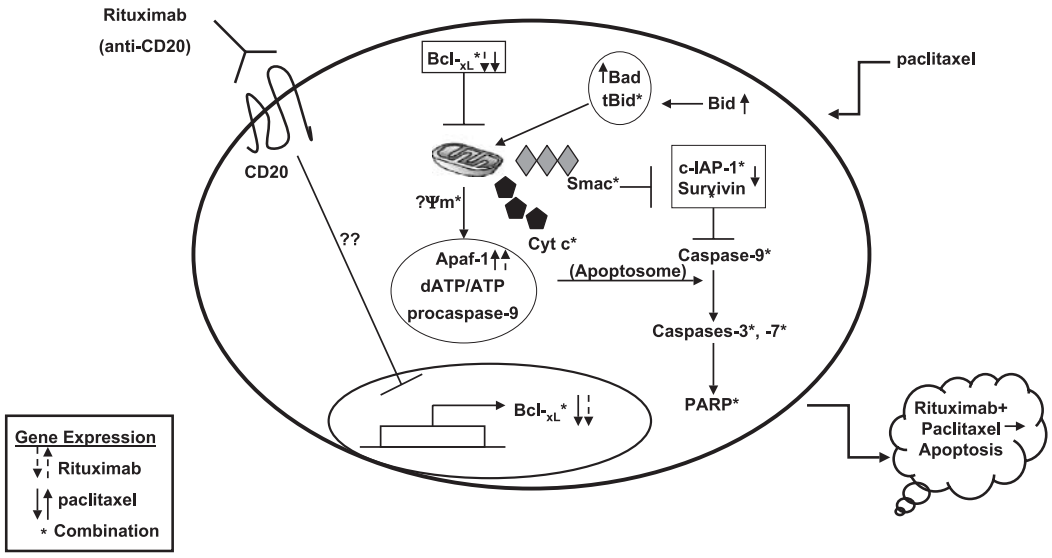

Figure 6. Proposed model of rituximab-mediated sensitization of Ramos cells to paclitaxel-induced apoptosis. On ligation to the B-cell restricted marker CD20, rituximab interferes with apoptosis signaling pathways via regulation of protein expression. The molecular events triggered by rituximab include decrease in the expression of the antiapoptotic protein Bcl-xL and the induction of the proapoptotic Apaf-1. Paclitaxel down-regulates the antiapoptotic proteins Bcl-xL and c-IAP-1 and up-regulates the expression of proapoptotic Bid and Apaf-1. Yet, these various modulatory effects by themselves are inadequate for the full induction of apoptosis. The combination treatment, via functional complementation, results in the formation of proapoptotic tBid and the induction of apoptosis. tBid migrates to and reside in the mitochondrial outer membrane. Decreased levels of Bcl-xL by rituximab and paclitaxel and the presence of tBid and high levels of Bad will alter the ratio of proapoptotic/antiapoptotic Bcl-2 family members. Decrease in this ratio, which is a key determinant in cellular fate in response to noxious stimuli, will collapse the $\Delta\psi_m$ and facilitate the release of apoptogenic molecules such as cytochrome *c* and Smac/DIABLO. Smac/DIABLO will bind to and repress the inhibitory effects of IAPs. Increased levels of Apaf-1 in combination with cytochrome *c* and dATP/ATP will facilitate the assembly of the apoptosome complex. Through autocatalytic processing, procaspase-9 becomes activated concurrently with decreased levels of certain IAPs and caspase-9 will activate caspase-3 and caspase-7 to subsequently cleave PARP and induce apoptosis. *Solid and dashed arrows,* the signaling molecules altered by paclitaxel and rituximab, respectively. *, Modulation by the combination treatment.

against chemotherapy (36–38). Therefore, modulation of the expression of IAPs shown here will decrease the apoptosis threshold and might contribute to the enhanced drug sensitivity of the NHL cells.

The combination treatment also resulted in the formation of tBid. When there is a block in the receptor-mediated signaling pathway (type I), small amounts of caspase-8 will cleave Bid. tBid will then migrate to and reside in the mitochondrial outer membrane, which will act as an amplification loop (39) for the induction of apoptosis. Thus, induction of Bad, formation of tBid (proapoptotic molecules), concurrence with the absence of Bcl-2, and complete abrogation of Bcl-xL (antiapoptotic molecules) will destabilize mitochondria. This notion is further supported by the observation that combination treatment resulted in decrease in $\Delta\psi_m$ (Table 4; Fig. 5D), cytosolic accumulation of cytochrome *c* and Smac/DIABLO (Fig. 5, C and E), subsequent activation of caspase-9, caspase-7, caspase-3, and PARP cleavage. Altogether, these findings favor the employment of the type II mitochondrial signaling pathway for the induction of apoptosis (40). Thus, the effects of rituximab and paclitaxel on the apoptotic signal transduction pathway suggest that each agent selectively modifies certain apoptotic gene products. Hence, rituximab complements and facilitates the cytotoxic activity of paclitaxel and the combination will result in the execution of apoptosis. The complementation model is schematically represented in Fig. 6.

The present findings emphasize the value of the complementation approach (Fig. 6) in the treatment of rituximab/drug-resistant NHL tumors cells. We suggest that the combination of a nontoxic agent such as rituximab and subtoxic concentrations of a chemotherapeutic drug such as paclitaxel, via selective regulation of expression of apoptosis-associated proteins, results in the reversal of resistance via synergy in apoptosis.

Acknowledgments

We thank Dr. Sara Huerta for assistance in the analysis of the apoptosis by assessing caspase-3 activity by flow cytometry, Kate Dinh for assistance in the preparation of this manuscript, and Golaun Odabaei for critical review of the manuscript.

References

1. Devesa, S. S. and Fears, T. Non-Hodgkin's lymphoma time trends: United States and International data. Cancer Res., *52:* 5432s–5440s, 1992.

2. Park, S. L., Tong, T., Bolden, S., and Wingo, P. A. Cancer statistics. CA Cancer J. Clin., *47:* 5–27, 1997.

3. White, C. A. Rituximab immunotherapy for non-Hodgkin's lymphoma. Cancer Biother. Radiopharm., *14:* 241–250, 1999.

4. Tedder, T. F. and Engel, P. CD20: a regulator of cell cycle progression of B lymhocytes. Immunol. Today, *15:* 450–454, 1994.

5. Shan, D., Ledbetter, J. A., and Press, O. W. Apoptosis of malignant human B cells by ligation of CD20 with monoclonal antibodies. Blood, *91:* 1644–1652, 1998.

6. Reff, M. E., Carner, K., Chambers, K. S., Chinn, P. C., Leonard, J. E.,

Raab, R., Newman, R. A., Hanna, N., and Anderson, D. R. Depletion of B cells in vivo by a chimeric mouse human monoclonal antibody to CD20. Blood, *83:* 435 – 445, 1994.

7. Coiffier, B., Haioun, C., Ketterer, N., Engert, A., Tilly, H., Ma, D., Johnson, P., Lister, A., Feuring-Buske, M., Radford, J. A., Capdeville, R., Diehl, R. V., and Reyes, F. Rituximab (anti-CD20 monoclonal antibody) for the treatment of patients with relapsing or refractory aggressive lymphoma: a multicenter phase II study. Blood, *92:* 1927 – 1932, 1998.

8. Grillo-Lopez, A. J., White, C. A., Varns, C., Shen, D., Wei, A., McClure, A., and Dallaire, B. K. Overview of the clinical development of rituximab: first monoclonal antibody approved for the treatment of lymphoma. Semin. Oncol., *26:* 66 – 73, 1999.

9. McLaughlin, P., Hagemeister, F. B., and Grillo-Lopez, A. J. Rituximab in indolent lymphoma: the single-agent pivotal trial. Semin. Oncol., *26:* 79 – 87, 1999.

10. Golay, J., Zaffaroni, L., Vaccari, T., Lazzari, M., Borleri, G-M., Bernasconi, S., Tedesco, F., Rambaldi, A., and Introna, M. Biologic response of B lymphoma cells to anti-CD20 monoclonal antibody rituximab in vitro: CD55 and CD95 regulate complement-mediated lysis. Blood, *95:* 3900 – 3908, 2000.

11. Shan, D., Ledbetter, J. A., and Press, O. W. Signaling events involved in anti-CD20 induced apoptosis of malignant human B cells. Cancer Immunol. Immunother., *48:* 673 – 683, 2000.

12. Ghetie, M. A., Bright, H., and Vitetta, E. S. Homodimers but not monomers of rituximab (chimeric anti-CD20) induce apoptosis inhuman B-lymphoma cells and synergize with a chemotherapeutic agent and an immunotoxin. Blood, *97:* 1392 – 1398, 2001.

13. Maloney, D. G., Smith, B., and Applebaum, F. R. The anti-tumor effect of monoclonal anti-CD20 antibody (mAB) therapy includes direct anti-proliferative activity and induction of apoptosis in positive non-Hodgkin's lymphoma (NHL) cell lines (Abstract). Blood, *88:* 637a, 1996.

14. Demidem, A., Lam, T., Alas, S., Hariharan, K., Hanna, N., and Bonavida, B. Chimeric anti-CD20 (IDEC-C2B8) monoclonal antibody sensitizes a B cell lymphoma cell line to cell killing by cytotoxic drugs. Cancer Biother. Radiopharm., *12:* 177 – 186, 1997.

15. Alas, S. and Bonavida, B. Rituximab inactivates STAT3 activity in B-non-Hodgkin's lymphoma through inhibition of the interleukin 10 autocrine/paracrine loop and results in down-regulation of Bcl-2 and sensitization to cytotoxic drugs. Cancer Res., *61:* 5137 – 5144, 2001.

16. Rowinsky, E. K. and Donehower, R. C. Antimicrotubule agents. *In:* B. A. Chabner and D. L. Longo (eds.). Cancer Chemotherapy and Biotherapy, 2nd ed. p. 263. Philadelphia, PA: Lippincott-Raven Publishers, 1996.

17. Yeung, T. K., Germond, C., Chen, X., and Wang, Z. The mode of action of Taxol: apoptosis at low concentration and necrosis at high concentration. Biochem. Biophys. Res. Commun., *263:* 398 – 404, 1999.

18. Goss, P., Stewart, A. K., Couture, F., Klasa, R., Gluck, S., Kaizer, L., Burkers, R., Charpentier, D., Palmer, M., Tye, L., and Dulude, H. Combined results of two phase II studies of Taxol (paclitaxel) in patients with relapsed or refractory lymphomas. Leuk. Lymph., *34:* 295 – 304, 1999.

19. Alas, A., Emmanouilides, C., and Bonavida, B. Inhibition of interleukin-10 by rituximab results in down-regulation of Bcl-2 and sensitization of B cell non-Hodgkin's lymphoma to apoptosis. Clin. Cancer Res., *7:* 709 – 723, 2001.

20. Haldar, S., Jena, N., and Croce, C. M. Inactivation of Bcl-2 by phosphorylation. Proc. Natl. Acad. Sci. USA, *92:* 4507 – 4511, 1995.

21. Klein, G., Giovanella, B., Westman, A., Stehlin, J. S., and Mumford, D. An EBV-genome-negative cell line established from an American Burkitt's lymphoma; receptor characteristics. EBV infectibility and permanent conversion into EBV-positive sublines by in vitro infection. Intervirology, *5:* 319 – 334, 1975.

22. Berinstein, N. L., Grillo-Lopez, A. J., White, C. A., Bence-Bruckler, I., Maloney, D., Czuczman, M., Green, D., Rosenberg, J., McLaughlin, P., and Shen, D. Association of serum rituximab (IDEC-C2B8) concentration and anti-tumor response in the treatment of recurrent low-grade or follicular non-Hodgkin's lymphoma. Ann. Oncol., *9:* 995 – 1001, 1998.

23. Nicoletti, I., Migliorati, G., Pagliacci, M. C., Grignani, F., and Riccardi, C. A rapid and simple method for measuring thymocyte apoptosis by propidium iodide staining and flow cytometry. J. Immunol. Methods, *139:* 271 – 279, 1991.

24. Perkins, C. L., Fang, G., Kim, C. N., and Bhalla, K. N. The role of Apaf-1, caspase-9, and Bid proteins in etoposide- or paclitaxel-induced mitochondrial events during apoptosis. Cancer Res., *60:* 1645 – 1653, 2000.

25. Jazirehi, A. R., Ng, C-P., Gan, X-H., Schiller, G., and Bonavida, B. Adriamycin sensitized the adriamycin-resistant 8226/Dox40 human multiple myeloma cells to Apo2L/TRAIL-mediated apoptosis. Clin. Cancer Res., *7:* 3874 – 3883, 2001.

26. Berenbaum, M. C. A method for testing for synergy with any number of agents. J. Infect. Dis., *137:* 122 – 130, 1978.

27. Tzung, S-P., Kim, C. M., Basanez, G., Giedt C. D., Simon, J., Zimmerberg, J., Zhang, K. Y. J., and Hockenbery, D. M. Antimycin A mimics a cell death-inducing Bcl-2 homology domain 3. Nat. Cell Biol., *3:* 183 – 191, 2001.

28. Jazirehi, A. R., Odabaei, G., Vega, M., Chatterjee, D., Goodglick, L., and Bonavida, B. Rituximab triggers RKIP expression and inhibits the ERK1/2 MAP kinase and AP-1 activation: role in down-regulation of Bcl-xL. Proc. Am. Assoc. Cancer Res., *44:* 1057 (R4610), 2003.

29. Liu, Q. Y. and Stein, C. A. Taxol and estramustine-induced modulation of human prostate cancer cell apoptosis via alteration in bcl-xL and bak expression. Clin. Cancer Res., *3:* 2039 – 2046, 1997.

30. Liu, J. R., Fletcher, B., Page, C., Hu, C., Nunez, G., and Baker, V. Bcl-xL is expressed in ovarian carcinoma and modulates chemotherapy-induced apoptosis. Gynecol. Oncol., *70:* 398 – 403, 1998.

31. Luo, D., Cheng, S. C., Xie, H., and Xie, Y. Effects of Bcl-2 and Bcl-xL protein levels on chemoresistance of hepatoblastoma Hep-G2 cell line. Biochem. Cell Biol., *78:* 119 – 126, 2000.

32. Ibrado, A. M., Huang, Y, Fang, G., and Bhalla, K. Bcl-xL overexpression inhibits Taxol-induced Yama protease activity and apoptosis. Cell Growth Differ., *7:* 1087 – 1094, 1996.

33. Strobel, T., Tai, Y. T., Korsmeyer, S., and Cannistra, S. A. BAD partly reverses paclitaxel resistance in human ovarian cancer cells. Oncogene, *17:* 2419 – 2427, 1998.

34. Perkins, C., Kim, C. N., Fang, G., and Bhalla, K. Overexpression of Apaf-1 promotes apoptosis of untreated and paclitaxel- or etoposide-treated HL-60 cells. Cancer Res., *58:* 4561 – 4566, 1998.

35. Moroni, M. C., Hickman, E. S., Denchi, E. L., Caprara, G., Colli, E., Cecconi, F., Muller, H., and Helin, K. Apaf-1 is a transcriptional target for E2F and p53. Nat. Cell Biol., *3:* 552 – 558, 2001.

36. Roy, N., Deveraux, Q. L., Takahashi, R., Salvesen, G. S., and Reed, J. C. The c-IAP-1 and c-IAP-2 proteins are direct inhibitors of specific caspases. EMBO J., *16:* 6914 – 6425, 1997.

37. Deveraux, Q. L., Roy, N., Stennicke, H. R., Arsdale, T. V., Zhou, Q., Srinivasula, S. M., Salvensen, G. S., and Reed, J. C. IAPs block apoptotic events induced by caspase-8 and cytochrome *c* by direct inhibition of distinct caspases. EMBO J., *17:* 2215 – 2223, 1998.

38. Tamm, I., Wang, Y., Sausville, E., Scidiero, D. A., Vigna, N., Oltersdorf, T., and Reed, J. C. IAP-family protein survivin inhibits caspase activity and apoptosis induced by Fas, Bax, caspases, and anti-cancer drugs. Cancer Res., *58:* 5315 – 5320, 1998.

39. Yin, X-M. Bid, a critical mediator of apoptosis induced by the activation of Fas/TNF-R1 death receptors in hepatocytes. J. Mol. Med., *78:* 203 – 211, 2000.

40. Waterhouse, N. J., Ricci, J. E., and Green, D. R. And all of a sudden it's over: mitochondrial outer-membrane permeabilization in apoptosis. Biochemie, *84:* 113 – 121, 2002.